

# Influence of scatter of cyclic properties of material on operational endurance of construction

V. Kliman<sup>1\*</sup>, M. Kepka<sup>2</sup>, J. Václavík<sup>3</sup>

<sup>1</sup>*Institute of Materials and Machine Mechanics, Slovak Academy of Sciences, Račianska 75, 831 02 Bratislava 3, Slovak Republic*

<sup>2</sup>*University of West Bohemia, Univerzitní 8, 306 14 Pilsen, Czech Republic*

<sup>3</sup>*Skoda Research s.r.o., Tylova 57, 316 00 Pilsen, Czech Republic*

Received 27 May 2010, received in revised form 16 August 2010, accepted 20 August 2010

## Abstract

In this study we propose a simple computing procedure to determine in probabilistic form the material constants that enter fatigue-life calculation, namely fatigue strength (ductility) coefficient  $\sigma'_f$ , ( $\varepsilon'_f$ ) and fatigue strength (ductility) exponent  $b$  ( $c$ ). The procedure, which assumes log-normal distribution of fatigue life on the  $S$ - $N$  curve, is based on the shift of the regression line (representing the fatigue-life curve) to the desired value of the probability of occurrence, and yields a set of material constants  $\sigma'_f$ ,  $b$ ,  $\varepsilon'_f$ ,  $c$  ranging in probability of occurrence from 1 % to 99 %. Suitable application of this procedure to the life estimation model under random loading conditions yields the fatigue-life distribution function taking into consideration the scatter of cyclic material properties.

The application of this method to evaluate fatigue reliability of a vehicle's construction is also presented. Based on the proposed methodology, the maximum permissible value of the scatter of a welded joint's cyclic properties was determined to ensure that the probability of premature fatigue failure occurrence would not exceed the allowable value.

**Key words:** material's cyclic properties, fatigue-life distribution function, probabilistic analysis, welded joint

## 1. Introduction

It is essential to ensure that material of construction is endowed with sufficient resistance against fatigue fracture even at the design stage. Therefore, there is need for a suitable method to assess whether the fatigue life of a designed construction ( $L_g$ , Fig. 1) is sufficiently greater than the desired operational endurance ( $L_{req}$ , Fig. 1).

Computing methods that employ the probabilistic approach to fatigue-life estimation are preferred for such assessments because in actual operation both material properties and construction loading are random in nature, i.e. the result of computational life estimation should be in the form of a distribution function. If it is necessary to modify the fatigue-life distribution function (FLDF) of the designed construction (Fig. 1) to fulfil the requirement  $L_g > L_{req}$ , usually

it is the material of the construction that has to be changed because it is not always possible to alter the operational loading to suit the design concept as such loading is governed by operational conditions. In this regard, the scatter of a material's mechanical properties plays a crucial role because the magnitude of the scatter could significantly affect the course of FLDF and consequently the conditions of reliable operation ( $L_g > L_{req}$  and  $P_g < P_a$ , Fig. 1).

In this article the emphasis is on development of a model for FLDF estimation that incorporates the scatter of material's mechanical properties at critical locations in the construction. Such a model of fatigue-life estimation enables assessment of the fatigue reliability of a construction in respect of the scatter of the material's cyclic properties and compares the different materials with respect to the desired values of  $L_{req}$  and  $P_a$  (Fig. 1). The model also, eventually, assesses from

\*Corresponding author: tel./fax: +421 2 59309417; e-mail address: [ummsklim@savba.sk](mailto:ummsklim@savba.sk)

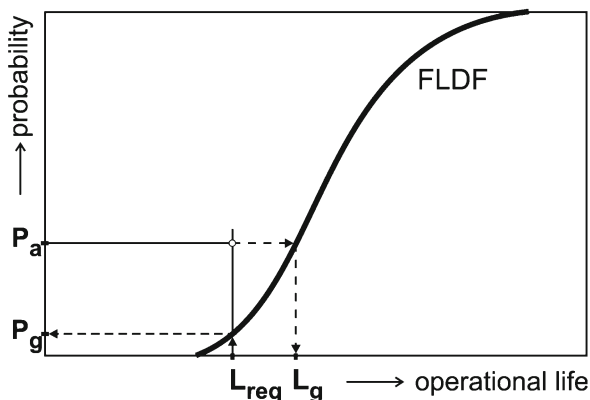


Fig. 1. Schematic illustration of the verification of fatigue life of construction design. FLDF – fatigue-life distribution function of designed construction;  $L_{req}$  – desired operational endurance of construction;  $P_a$  – permissible probability of occurrence of premature fatigue failure;  $L_g$  – operational endurance for admissible value of  $P_a$ , confirmed by the calculated FLDF;  $P_g$  – probability of occurrence of premature fatigue failure, confirmed by the calculated FLDF for the  $L_{req}$  value.

this standpoint the influence of other factors, such as heat treatment, welding technology, etc.

Therefore, this paper proposes:

- a simple computing method to enable determination, in probabilistic form, of the material characteristics needed for fatigue-life calculation,
- applying this method in the model to estimate the operational fatigue life (and thereby obtaining the FLDF of the construction regarding the material's cyclic properties' scatter), and
- practical application of the proposed methodology to evaluate the operational reliability of the construction of an urban vehicle from the material's fatigue perspective.

## 2. Probabilistic interpretation of material characteristics

To calculate the fatigue damage at the critical spot in a construction (that is, the location where the fatigue failure could be expected as a result of the action of variable stress), the behavioural characteristics of the material under cyclic loading are needed. In the fatigue-life estimation model, which is based on the “local stress or strain concept”, the material constants that represent these characteristics are the parameters of the following fatigue-life curves:

- Manson-Coffin's fatigue-life curve [1, 2]:

$$\varepsilon_a = \frac{\sigma'_f}{E}(2N_f)^b + \varepsilon'_f(2N_f)^c, \quad (1)$$

- Wöhler's curve:

$$\sigma_a^m N_f = K = \text{const}, \quad (2)$$

- or parameters of the so-called rewritten Wöhler's curve in the form of Basquin's [3] equation:

$$\sigma_a = \sigma'_f(2N_f)^b, \quad (3)$$

where  $\sigma_a$  is the stress amplitude,  $\varepsilon_a$  is the total strain amplitude,  $N_f$  is number of cycles to fatigue failure,  $\sigma'_f$  is fatigue strength coefficient,  $b$  is fatigue strength exponent,  $\varepsilon'_f$  is fatigue ductility coefficient,  $c$  is fatigue ductility exponent.

The following relations are valid between the parameters of Eqs. (2) and (3):

$$b = -\frac{1}{m}; \quad \sigma'_f = (2K)^{1/m}. \quad (4)$$

The material constants  $\sigma'_f$ ,  $b$ ,  $\varepsilon'_f$ ,  $c$  then represent the cyclic properties of the material and are determined based on linear regression using experimental dependence  $N_f = f(\sigma_a)$  and  $N_f = f(\varepsilon_a)$ .

The values of the constants  $\sigma'_f$ ,  $b$ ,  $\varepsilon'_f$ ,  $c$ , obtained by regression analysis, correspond to the 50 % probability of occurrence (their table values for different materials are readily available, e.g. in [4, 5]). However, in reality material properties are random in nature. The

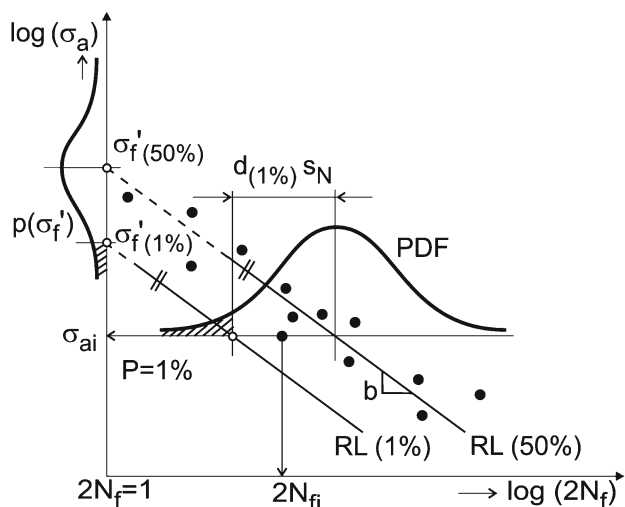


Fig. 2. Scheme for determination of the material constants ( $\sigma'_f$ ,  $b$ ) for  $P(\%)$  probability of occurrence. • – fatigue-life curve experimental points ( $\sigma_{ai}$ ;  $2N_{fi}$ ); RL(50%) – regression line; RL(1%) – regression line shifted to the value of  $P = 1\%$ ;  $s_N$  – standard deviation;  $d_{(1\%)}$  – multiple of standard deviation determining the value of  $P = 1\%$ ; PDF – probability density function (log-normal distribution of  $N_f$ ).

degree of this randomness is given by the magnitude of the scatter of experimental points along the regression line, representing the fatigue-life curve of the material at the critical spot in a construction (CSC) (see Fig. 2 and Fig. 4). In fact, any of these experimental points could represent the cyclic material properties of the CSC investigated. This means that in practice the computational estimations of fatigue damage, obtained by employing solely the parameters of the regression line, could be overestimated or underestimated depending upon mutual positions of the regression line and the experimental point representing cyclic material properties of the CSC investigated. Therefore, in fatigue damage calculations material properties have to be interpreted probabilistically. Adopting this approach for determination of material constants allows the calculation of the fatigue life of the CSC investigated in the form of a distribution function incorporating the scatter in the material's cyclic properties.

The material constants  $\sigma'_f, b, \varepsilon'_f, c$  for the different probabilities of occurrence are computed employing a set of fatigue-life curve experimental points (Fig. 2) assuming the following:

- the life (that is the number of cycles to fatigue failure  $N_f$ , for loading with a harmonic cycle of amplitude  $\sigma_a$ ) has log-normal distribution, and

- the values of the material constants ( $\sigma'_f, b, \varepsilon'_f, c$ ) for the  $P\%$  probability of occurrence (hereafter  $P\%$ ) are obtained based on the shift of the regression line to the desired value of  $P\%$ .

This principle is schematically depicted for Basquin's relation in Fig. 2. From the set of experimental points  $(\sigma_{ai}; 2N_{fi})_{i=1}^n$ , for the fatigue-life curve in the form of Eq. (3), the set of material constants ( $\sigma'_f, b$ ) for the  $P\%$  ranging from 1 % to 99 % are obtained in this manner. It is evident from Fig. 2 that according to this methodology, while only the value of the fatigue strength coefficient  $\sigma'_f$  is a function of  $P\%$ , the value of  $b$  remains unchanged for all values of probability.

When utilizing the set of fatigue-life curve experimental points  $(\sigma_{ai}; 2N_{fi})_{i=1}^n$  to determine the regression line in accordance with the scheme in Fig. 2, the stress amplitude  $\sigma_a$  must be considered as an independently variable and the number of cycles to failure  $N_f$  as dependently variable. Therefore, it is necessary to perform linear regression in the coordinate system  $(2N_f) = f(\sigma_a)$ . Then, based on Eq. (3), the regression line equation assumes the form

$$\log(2N_f) = -\frac{1}{b} \log \sigma'_f + \frac{1}{b} \log \sigma_a. \quad (5)$$

Statistical evaluation of the set of  $n$  experimental points  $(\sigma_{ai}; 2N_{fi})_{i=1}^n$  leads to the regression line equation assuming the form

$$\log(2N_f) = A_0 + B_0 \log \sigma_a, \quad (6)$$

whereby, with respect to Eq. (5), the following relations are valid between the parameters sought  $\sigma'_f, b$ , and the constants evaluated  $A_0, B_0$ :

$$B_0 = \frac{1}{b} \quad (7a)$$

and

$$A_0 = -\frac{1}{b} \log \sigma'_f. \quad (7b)$$

The values of parameters  $(\sigma'_f, b)$  of the material for 50 % probability of occurrence are then obtained based on the already known values of constants  $A_0$  and  $B_0$  by means of the following relations

$$B_0 = \frac{1}{b} \Rightarrow b = \frac{1}{B_0}, \quad (8a)$$

$$A_0 = -\frac{1}{b} \log \sigma'_f \Rightarrow \sigma'_f = 10^{-bA_0}. \quad (8b)$$

The equation of the regression line that was shifted is as follows:

$$\log(2N_f) = A_0 \pm d_{(P\%)} s_N + B_0 \log \sigma_a, \quad (9)$$

where  $d_{(P\%)}$  is the constant expressing the regression line shift (in multiples of the  $s_N$  standard deviation) to the required value of  $P\%$ . For  $P = 50\%$  the value  $d_{(50\%)} = 0$ . The signs  $(-)$  and  $(+)$  are valid for determination of the lower and upper interval limits, respectively, of the confidence interval. The values of the constant  $d_{(P\%)}$  for some probabilities ( $P\%$  in Fig. 2) are noted in the Appendix.  $s_N$  is the standard deviation of the distribution of number of cycles to failure  $N_f$ .

For the set of  $n$  experimental points  $(\sigma_{ai}; 2N_{fi})_{i=1}^n$ , the  $s_N$  is given by the following relation

$$s_N = \sqrt{\frac{\sum_{i=1}^n Y_i^2 - A_0 \sum_{i=1}^n Y_i - B_0 \sum_{i=1}^n X_i Y_i}{n - 2}}, \quad (10)$$

where  $Y = \log(2N_f)$ ,  $X = \log \sigma_a$ , and the constants  $A_0, B_0$  are regression line parameters in Eq. (6).

It follows from the above-noted assumption that the material constant  $b$  will remain unchanged for all values of  $P\%$ . The value of  $\sigma'_{f(P\%)}$ , for  $P\%$  is obtained using the evaluated constant  $A_0$  (Eq. 6) and the relevant value of the  $d_{(P\%)}$  constant.

Let us note

$$A_0 \pm d_{(P\%)} s_N = A_1. \quad (11)$$

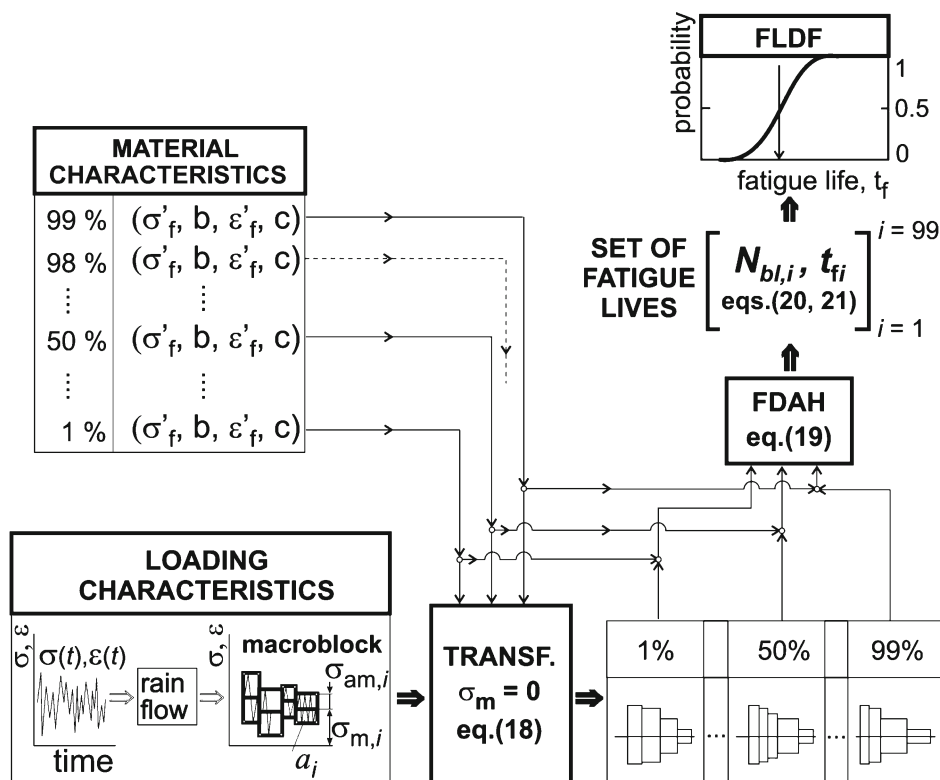


Fig. 3. Layout of detailed procedure for fatigue-life distribution function (FLDF) calculation in respect of the scatter of cyclic material properties. FDAH – fatigue damage accumulation hypothesis;  $t_f$  – fatigue life expressed in terms of time;  $N_{bl}$  – fatigue life expressed by the number of macroblock repetitions;  $\sigma(t)$  – operational loading process.

Equation (9) of the shifted regression line then becomes

$$\log(2N_f) = A_1 + B_0 \log \sigma_a. \quad (12)$$

With respect to Eqs. (5), (6), and (11)

$$A_1 = -\frac{1}{b} \log \sigma'_{f(P\%)}, \quad (13)$$

and the sought value of the fatigue strength coefficient for  $P\%$

$$\sigma'_{f(P\%)} = 10^{-bA_1} = 10^{-b(A_0 \pm d(P\%)SN)}. \quad (14)$$

By the same procedure, it is possible to obtain in probabilistic form the set of material constants pertaining to Manson-Coffin's or Wöhler's curve. Let us also note that the assumption of log-normal distribution of fatigue life, used in our derivations, is a widely accepted practice, e.g. by the British Standard BS 7608 [6], for determination of standardized  $S$ - $N$  curves.

### 3. Fatigue-life estimation model

In fatigue-life calculation it is necessary to consider the occurrence of all possibilities of cyclic material

properties, i.e. in a fatigue-life estimation model we have to take into consideration the parameters of the shifted fatigue-life curves for all probabilities of occurrence (from 1 % to 99 %). The schematic presentation of the detailed procedure for calculation of FLDF, in respect of the scatter of cyclic properties of the material, is given in Fig. 3.

The principle underlying this calculation is the transformation of the  $\sigma(t)$  random loading process into the macroblock of harmonic cycles (a set of harmonic cycles with different  $\sigma_{am}$  amplitudes and  $\sigma_m$  mean values) which, together with the material characteristics, represents the input to the fatigue-damage accumulation hypothesis (FDAH). Based on an adequate FDAH that correlates both the material- and loading characteristics, the fatigue life is then calculated and expressed in the number of macroblock repetitions  $N_{bl}$ , or directly in terms of time  $t_f$  (see Section 4). This procedure actually combines the evaluated macroblock with material parameters for  $P\%$  from 1 % to 99 %, i.e. 99 combinations enter the FDAH (when the interval limit rises by 1 %). The calculation output is a set of 99 feasible values of lives serving as the fatigue-life distribution function (FLDF) calculation.

It should be noted that to obtain the representative FLDF, the probabilities of occurrence must be raised by constant values of  $P\%$ . Mostly, it is sufficient to

raise the probabilities by intervals of 0.5 % or 1 %.

The length of operational life calculated according to the scheme in Fig. 3 is also influenced by some other factors:

- *Selection of FDAH.* The Palmgren-Miner’s [7, 8] hypothesis is most frequently used, mainly for its simplicity. The simple- and physico-supported hypothesis (that the fatigue damage is characterized by plastic strain energy) according to [9] could also be recommended. Nevertheless, it is always advisable to apply all the available FDAHs in the calculation of life. A survey of FDAHs is available in [10].

- *Method of transformation* of the random loading process into a macroblock of harmonic cycles. For fatigue analysis, the application of the so-called “rainflow method” [11] is appropriate. The method stems from decomposition of the random loading process into a set of harmonic cycles based on closed hysteresis loops. While there are several algorithms for selection of harmonic cycles from the  $\sigma(t)$  random process, the standardized method [12] is recommended.

- *Operational loading process record.* The loading process is mostly obtained by strain gauge measurements in the form of time-dependent strain  $\varepsilon(t)$ . The measured record of loading must be representative and sufficiently long, i.e. must include all the significant service operations of the construction. The minimum record length needed for the representative fatigue-life calculation is given by the statistical criteria for evaluation of the loading process characteristics [13].

- The effect of *mean value.* There are several models for study of mean stress effect in fatigue-life calculations [14–18]. These models are used to transform the macroblock, obtained by the rainflow method in the form of harmonic cycles with mean values, into a set of harmonic cycles with zero mean value (Fig. 3). A survey and comparison of the individual models are found in [19–25]. The most frequently used is the model according to Morrow [14] (reduction of the  $\sigma'_f$  coefficient by the  $\sigma_m$  value) and the so-called SWT parameter [18] ( $\sigma_{\max}\Delta\varepsilon/2$ ), and their eventual modifications [26, 27].

- *Amplitudes below the fatigue limit.* The influence of amplitudes below the fatigue limit ( $\sigma_C$ ) on calculated life is rather small and the amplitudes  $\sigma_a < (0.5\div 0.7)\sigma_C$  are usually omitted [28] in fatigue damage analysis. To include the  $\sigma_a < \sigma_C$  in fatigue-life calculations, it is necessary to employ the parameters of the fatigue-life curve extrapolated below the fatigue limit  $\sigma_C$ .

#### 4. Example of application

Potentialities of the estimation model of fatigue-life distribution function (FLDF), presented in Section 3, are demonstrated here by evaluating the fatigue reli-

ability of an urban vehicle’s construction. The magnitude of the scatter of cyclic properties is an important parameter in fatigue reliability evaluation because it could considerably affect the shape of the FLDF calculated of the CSC and, subsequently, also of the probability value of premature fatigue failure  $P_g$  (Fig. 1).

In this case, the welded joint represents the critical spot in the construction (CSC). The magnitude of the scatter of the welded joint’s cyclic properties primarily depends on the method of welding employed, inhomogeneity of the mechanical properties of the basic and added materials, the presence and quantity of various defects arising during welding, compliance with requirements of the welding process, and other factors. Therefore, fatigue assessment of welded joints is a very real problem [29] and recent developments in local assessment concepts are given in [30]. The specific aim of this part of the paper was to investigate the magnitude of influence the scatter of the welded joint’s cyclic properties yields on fatigue life and thereby assess the resistance of the vehicle’s construction to fatigue failure.

To assess the fatigue resistance of the vehicle’s construction, it is necessary to calculate the FLDF of the welded joint and compare it with the requirement for failure-free operation ( $L_{\text{req}}, P_a$ , Fig. 1) of the construction. To calculate the FDLF (following the method detailed in Fig. 3) it is necessary:

- to transform the load acting at the CSC into the macroblock of harmonic cycles using the “standardized rainflow method [12]”, and

- to determine the set of material constants that represent the cyclic properties of the welded joint, i.e. to compute the values of these constants for the probabilities of occurrence ranging from 1 % to 99 %.

#### 4.1. Determination of material characteristics representing the cyclic properties of the welded joint

Following the methodology detailed in Section 2, the material constants entering the fatigue-life calculation were determined based on fatigue-life test results. Test specimen, representing the welded joint at the CSC, is illustrated in the inset of Fig. 4. The fatigue tests were conducted under loading mode with  $\sigma_a = \text{const}$ . The stress amplitude was  $\sigma_a = F_a/s_1 \times s_2 = F_a/5 \times 100$ . The results obtained are presented in Table 1 and are depicted in the form of fatigue-life curves in Fig. 4.

The following regression line equation (in the form of Eq. (6)) was obtained by statistical treatment of the experimental results presented in Table 1:

$$\log(2N_f) = 12.6355 - 4.36284(\log \sigma_a). \quad (15)$$

The fatigue-life curve for 50 % probability of occur-

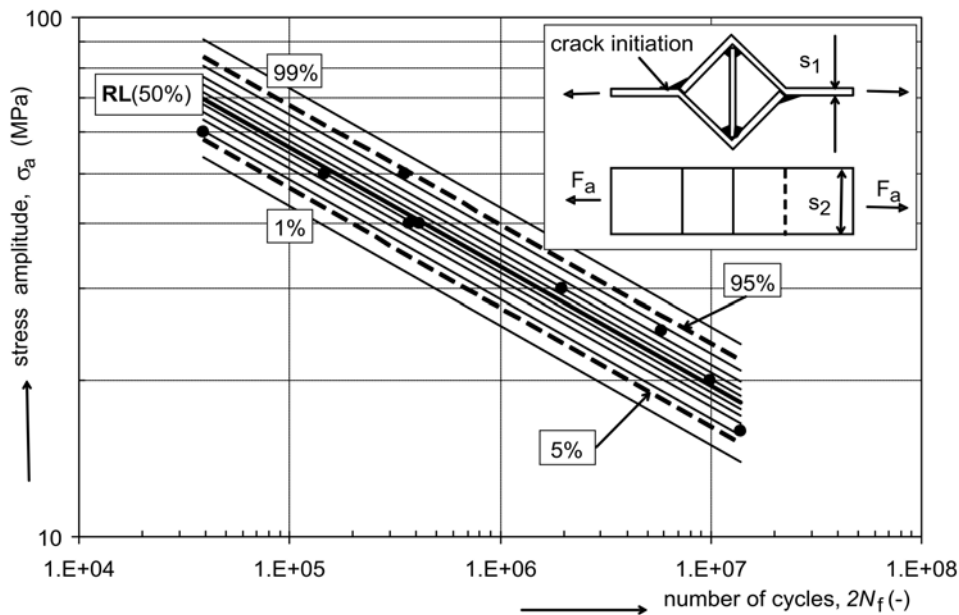


Fig. 4. Fatigue-life curves of the critical spot of the vehicle's construction calculated for different probabilities of occurrence,  $P\%$ . RL(50%) – regression line, Eq. (16); RL(5%) – shifted fatigue-life curve (lower tolerance limit for 90 % confidence interval), (Fig. 2); RL(95%) – shifted fatigue-life curve (upper tolerance limit for 90 % confidence interval); ● – experimental points  $(\sigma_{ai}; 2N_{fi})_{i=1}^9$ .

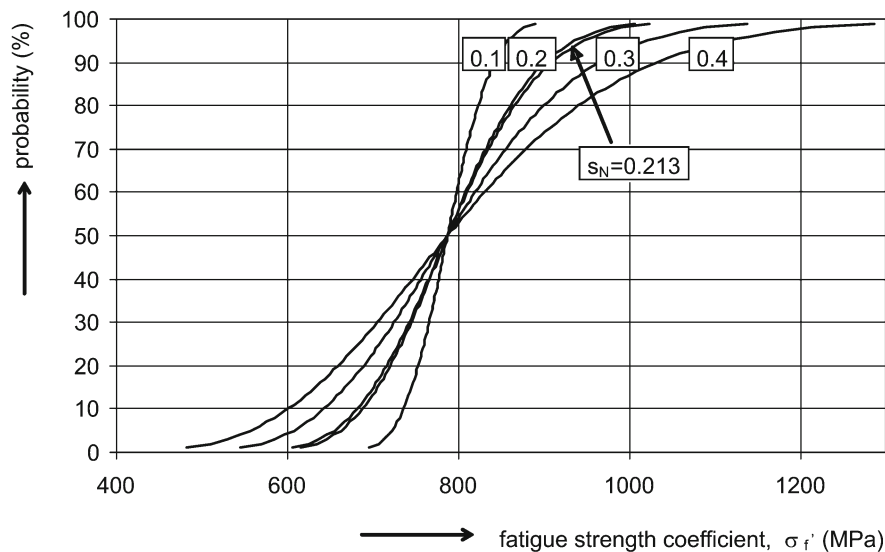


Fig. 5. Fatigue strength coefficient ( $\sigma'_f$ ) as a function of probability of occurrence ( $P\%$ ) and standard deviation ( $s_N$ ). 0.213 – real value of standard deviation  $s_N$ ; (0.1, 0.2, 0.3, 0.4) – simulated values of standard deviation  $s_N$ .

rence in the form of Basquin's relation, RL(50%), is shown in Fig. 4. The values of the material constants  $\sigma'_f$  and  $b$  were obtained applying Eq. (8):

$$\sigma_a = \sigma'_f (2N_f)^b = 787.34 (2N_f)^{-0.22921}. \quad (16)$$

The value of standard deviation  $s_N$ , (calculated according to Eq. (10)), for the set of experimental points (Table 1) in the form  $(\sigma_{ai}; 2N_{fi})_{i=1}^9$ , is  $s_N = 0.213$ .

Figure 4 also shows the set of fatigue-life curves (shifted regression lines), calculated for different  $P\%$  based on Eq. (9) for the value of  $s_N = 0.213$ . The corresponding values of material constants  $\sigma'_f$ , computed for  $P\%$  from 1 % to 99 % using Eq. (14), are presented in the form of function  $\sigma'_f = f(P\%)$  in Fig. 5, and for some probabilities also in the Appendix. The value of the fatigue strength exponent  $b = -0.22921$ , following the methodology presented in Section 2, remains unchanged for all values of  $P\%$ . The functions

Table 1. Fatigue test results

No.	$\sigma_a$ (MPa)	$N_f$ (-)
1	60	19500
2	50	73100
3	50	176200
4	40	184300
5	40	207600
6	30	985200
7	25	2895300
8	20	4956100
9	16	6958400

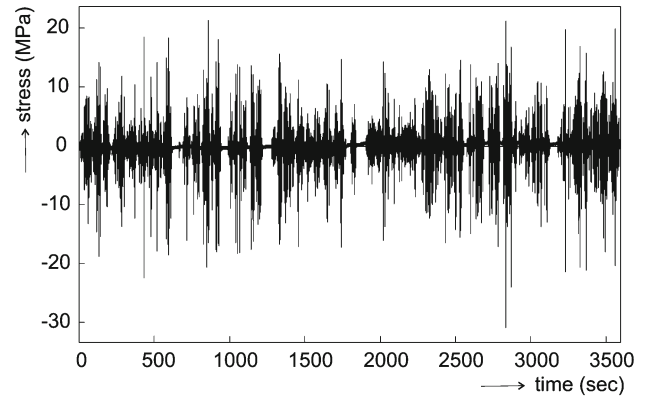


Fig. 6. Data on the  $\sigma(t)$  loading process.

$\sigma'_f = f(P\%)$  in the form of graphs, calculated for other (simulated) values of standard deviation, are also presented in Fig. 5.

**4.2. Loading process**

Data typical of the loading process were obtained by strain-gauge measurement at the critical spot of the vehicle’s construction and recorded on a drive along the road on the normal service route (a closed circle of circumference 19.2 km). The strain gauge was located on the smooth part of the construction near the weld so that the loading process was recorded in the direction of the principal stress. The typical loading process in the form of time-dependent stress  $\sigma(t)$  is shown in Fig. 6, and its characteristics are presented in Table 2.

To estimate the fatigue-life of the CSC adopting the scheme detailed in Fig. 3, the  $\sigma(t)$  loading process was transformed into the set of harmonic cycles (macroblock) using the standardized rainflow method [12].

**4.3. Fatigue-life calculation and analysis of the influence of the scatter of cyclic material properties on fatigue reliability**

In fatigue-life calculation (as per the method detailed in Fig. 3) of the CSC, the Palmgren-Miner (P-M) [7, 8] *fatigue damage accumulation hypothesis*

was used:

$$\sum_{(i)} \frac{a_i}{N_{fi}} = 1, \tag{17}$$

where  $a_i$  is the number of  $\sigma_{ai}$  stress amplitudes in the loading macroblock, obtained by the rainflow method from the  $\sigma(t)$  loading process,  $N_{fi}$  is the number of cycles to fatigue failure corresponding to the loading with  $\sigma_{ai}$  amplitude.  $N_{fi}$  is determined applying Eq. (3).

The effect of mean stress  $\sigma_m$  is evaluated according to Morrow’s concept [14]. The corresponding relation between the  $\sigma_a$  stress amplitude (for the cycle with  $\sigma_m = 0$ ) and the  $\sigma_{am}$  stress amplitude (for the cycle with  $\sigma_m \neq 0$ ) is utilized in the form

$$\sigma_{am} = \sigma_a \left( 1 - \frac{\sigma_m}{\sigma'_f} \right). \tag{18}$$

According to Palmgren-Miner [7, 8], the fatigue damage  $D$  caused by one macroblock, i.e., induced by the  $\sigma(t)$  random loading process of length  $t_s = 3596.37$  s (time segment of the  $\sigma(t)$  process, in Fig. 6 above, from which the macroblock of harmonic cycles was obtained by the rainflow method), is given by the following relation:

$$D = \sum_{(i)} \frac{a_i}{N_{fi}}. \tag{19}$$

Table 2. Loading process characteristics

	Maximum stress (MPa)	Minimum stress (MPa)	Mean value (MPa)	Median (MPa)	Standard deviation (MPa)	Number of ordinates	Sample frequency (Hz)
$\sigma(t)$	21.18	-30.94	-0.21	-0.179	1.858	1 438 550	400

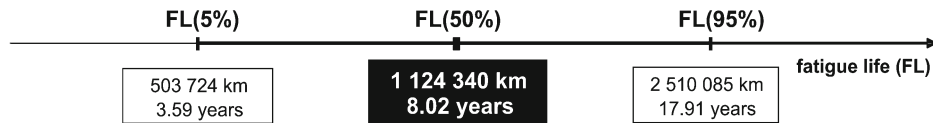


Fig. 7. Fatigue life (FL) for 90 % confidence interval (standard deviation  $s_N = 0.213$ ). FL(50%) – fatigue life calculated for the regression line material parameters (Fig. 4); FL(5%) – fatigue life corresponding to the lower limit of 90 % confidence interval (calculated for the parameters of RL(5%) shifted fatigue-life curve, Fig. 4); FL(95%) – fatigue life corresponding to the upper limit of 90 % confidence interval (calculated for the parameters of RL(95%) shifted fatigue-life curve, Fig. 4).

Fatigue life, expressed by the number of macroblock repetitions ( $N_{bl}$ ), is a result of the limit state condition, Eq. (17), i.e.

$$N_{bl}D = 1 \Rightarrow N_{bl} = D^{-1}. \quad (20)$$

The fatigue life  $N_{bl}$  so calculated is transformed back to the time domain using the following relation:

$$t_f = N_{bl}t_s, \quad (21)$$

where  $t_f$  is fatigue life expressed in terms of time,  $t_s$  is the time segment of the  $\sigma(t)$  loading process, from which the macroblock was obtained.

#### 4.3.1. Influence of the scatter of cyclic properties of the welded joint on fatigue life – analysis by means of confidence intervals

The analysis involves determining the expected fatigue-life span (in the context of the scatter of cyclic properties of the welded joint) of the CSC for the desired probability of occurrence. The value of the desired probability of occurrence selected was 90 %. This means that for calculation of fatigue-life limit values (the lower and upper limits of the 90 % confidence interval) material constants  $\sigma'_f$ ,  $b$  for  $P\%$  of 5 % and 95 % are needed (see also Fig. 2). Fatigue life is computed as per the diagram in Fig. 3, employing Eqs. (17) through (21), for the parameters of the RL(50%) regression line and for those of the shifted regression lines RL(5%) and RL(95%), Fig. 4. The results of calculation of life span are illustrated in Fig. 7.

##### Details of calculation:

– loading input (Fig. 3): 1 macroblock obtained by the rainflow method [12] from the entire record of the  $\sigma(t)$  loading process in Fig. 6;

– material input:

$\sigma'_f = 787.34$  MPa,  $b = -0.22921$ , which are parameters of the RL(50%) regression line (Fig. 4, Eq. (16));

$\sigma'_f(5\%) = 654.77$  MPa,  $b(5\%) = -0.22921$ , which are parameters of the RL(5%) shifted regression line (Fig. 4 and Appendix);

$\sigma'_f(95\%) = 946.73$  MPa,  $b(95\%) = -0.22921$ , which are parameters of the RL(95%) shifted regression line (Fig. 4 and Appendix);

– data for converting of life calculated in “hours” into life expressed in “km” and “years” of operation:

the  $\sigma(t)$  loading process – 1 circle: 19.2 km,  $t_s = 3596.37$  s

average speed: 19.2193 km/hour

operation: 20 circles/day

The results in Fig. 7 show that, consequent to the scatter of cyclic properties of the welded joint, the fatigue life of CSC that could be expected with 90 % probability would range from 3.59 years to 17.91 years. In terms of fatigue reliability, this means that with probability of 5 % the actual fatigue life of the welded joint could be less than 3.59 years. The span of the 90 % interval depends on the magnitude of the scatter of experimental points around the regression line (Fig. 4), i.e. on the value of standard deviation  $s_N$ . This dependence is evident from Fig. 8 and Table 3, which show the fatigue lives corresponding to the lower and upper limits of the 90 % confidence interval calculated for various values of standard deviation  $s_N$ .

It follows from the Fig. 8 that only a welded joint with maximum value of standard deviation  $s_N = 0.12$  could guarantee 5 years of operational endurance ( $L_{req}$ , Fig. 1) when the permissible probability of occurrence of premature fatigue failure is 5 % ( $P_a$ , Fig. 1). In such a case, the expected fatigue life of the critical spot of the vehicle construction will be in the range 5 to 13 years with the probability of 90 %. However, for the present value of scatter (with  $s_N = 0.213$ ) and for the requirement of 5 years, the probability of premature fatigue failure occurrence is  $X\%$ , i.e. it is greater than the permissible value of 5 %.

#### 4.3.2. Influence of scatter of welded joints' cyclic properties on fatigue life – analysis by means of fatigue-life distribution function

More information about the influence of the scatter of welded joints' cyclic properties on fatigue life of CSC could be gathered by analysing the FLDF calculations for various magnitudes of the scatter. Besides determining the expected span of fatigue life, such an analysis enables definition of the distribution of fatigue life in this interval. FLDF in respect of the scatter of cyclic material properties is calculated as per the procedure detailed in Fig. 3.



Table 3. Fatigue-life limit values calculated for 90 % confidence interval and for simulated values of standard deviation  $s_N$ . (0.1, 0.2, 0.3, and 0.4) are the simulated values of standard deviations; 0.213 is the real standard deviation

Standard deviation $s_N$	FL(5%) (years)	FL(95%) (years)	$\sigma'_f$ (5%) (MPa)	$\sigma'_f$ (95%) (MPa)	$b$ (-)
0.100	5.50	11.70	722.05	858.52	-0.22921
0.200	3.77	17.05	662.19	936.14	-0.22921
<b>0.213</b>	<b>3.59</b>	<b>17.91</b>	<b>654.77</b>	<b>946.73</b>	<b>-0.22921</b>
0.300	2.59	24.86	607.28	1020.78	-0.22921
0.400	1.78	36.25	556.93	1113.06	-0.22921

Table 4. Characteristics of calculated FLDFs (Fig. 9)

Fatigue-life distribution function (FLDF)				
Standard deviation on $S-N$ curve	Mean value (years)	Standard deviation (years)	Minimum value (years)	Maximum value (years)
0.100	8.22	1.83	4.70	13.71
0.200	8.84	4.01	2.75	23.42
<b>0.213</b>	<b>8.95</b>	<b>4.34</b>	<b>2.56</b>	<b>25.11</b>
0.300	9.96	6.99	1.61	40.02
0.400	11.74	11.43	0.94	68.40

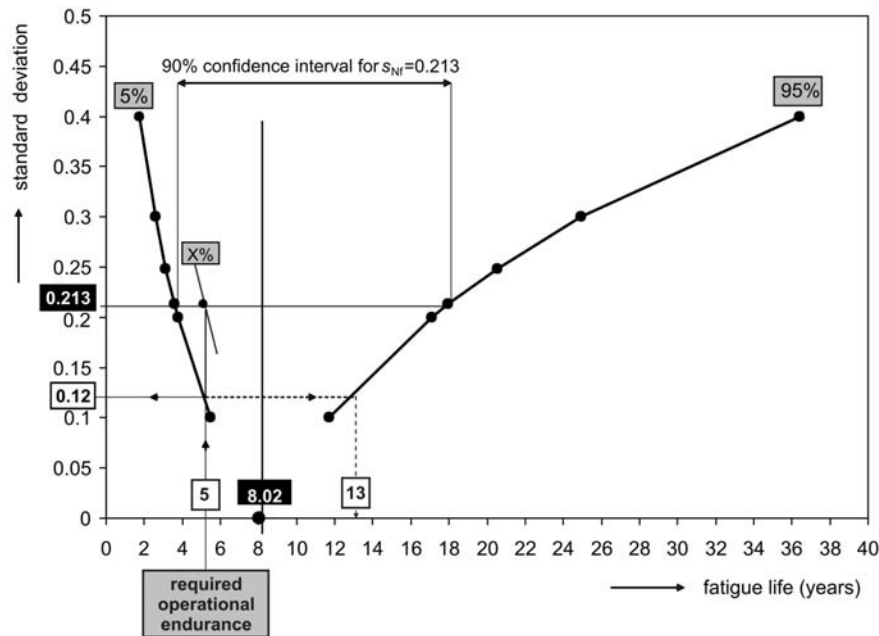


Fig. 8. Fatigue life with 90 % confidence interval calculated for different values of standard deviation  $s_N$ .

The data needed to be entered in the model for calculating FLDF are:

– loading input (Fig. 3): 1 macroblock obtained by the rainflow method [12] from the entire record of the  $\sigma(t)$  loading process in Fig. 6;

– material input: the set of material constants ( $\sigma'_f$ ,  $b$ ), computed for  $P\%$  from 1 % to 99 % using Eq. (14).

FLDFs, calculated for the real standard deviation  $s_N = 0.213$  as well as for the simulated values of  $s_N = 0.1, 0.2, 0.3,$  and  $0.4$ , are shown in Fig. 9. Parameters of the individual FLDFs, plotted in Fig. 9, are given in Table 4.

Figure 9 shows that it is now possible to read the  $X\%$  value (appearing in Fig. 8) directly from the FLDF calculated for the  $s_N = 0.213$ , i.e. the value

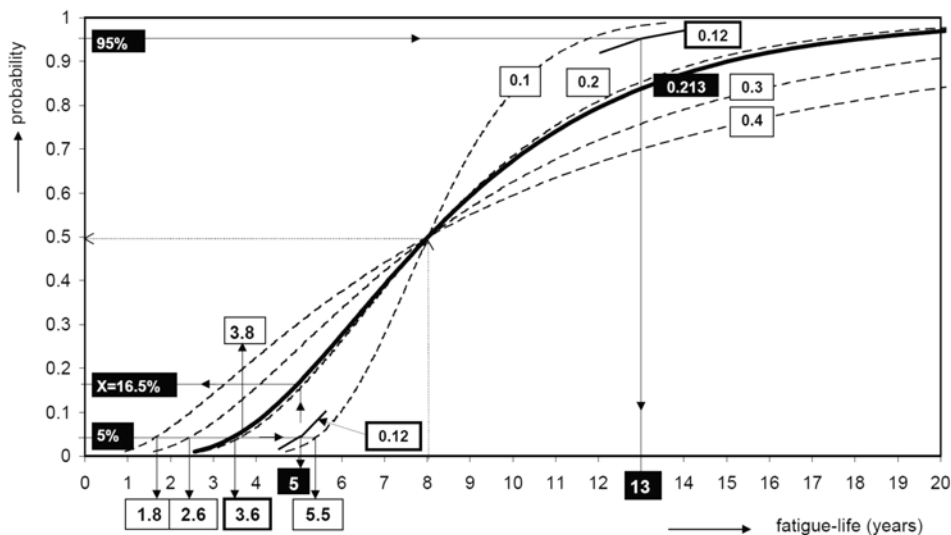


Fig. 9. Fatigue-life distribution function, representing the stochastic nature of cyclic material properties at the critical spot of the construction, calculated for different magnitudes of the scatter of fatigue-life curve experimental points (Fig. 4). **0.213** – real value of standard deviation  $s_N$  (Eq. 10); **0.1**, **0.2**, **0.3**, **0.4** – simulated values of standard deviation; **5 years** – required operational endurance ( $L_{req}$ , Fig. 1); **5%** – permissible probability of premature fatigue failure occurrence ( $P_a$ , Fig. 1).

$X = 16.5\%$ . In practice, this means that in the case of our vehicle ( $s_N = 0.213$ ) the probability of premature fatigue failure occurring (i.e. before expiry of the desired 5 years of failure-free operation) is 16.5%. It is also apparent from Fig. 9 that the magnitude of scatter greatly influences the guaranteed fatigue life ( $L_g$ , Fig. 1) of the CSC. For instance, for the 5% probability of fatigue-failure occurrence the guaranteed fatigue life ( $L_g$ ) varies from 1.8 to 5.5 years, depending upon the magnitude of the scatter (represented by the value of standard deviation  $s_N$ ) of the welded joint's cyclic properties. For a 5% probability of fatigue failure, we can guarantee in our case (where  $s_N = 0.213$ ) a fatigue life of only 3.6 years, whereby, in respect of the requirement  $L_{req} = 5$  years, the standard deviation  $s_N$  should be 0.12. It follows from the above-noted that in our case the CSC do not fulfil the condition of reliable operation for the required values of  $(L_{req}; P_a) = (5 \text{ years}; 5\%)$ , because for the  $L_{req} = 5$  years the value of  $P_g = 16.5\% > P_a = 5\%$ , and for the  $P_a = 5\%$  the value of  $L_g = 3.6 \text{ years} < L_{req} = 5 \text{ years}$ .

## 5. Discussion

It should be stressed that in the model of life estimation presented, fatigue failure is defined as the time required initiating a crack of  $\sim 1$  mm in length, i.e. the time required for the so-called engineering initiation of fatigue crack. Owing to the precision in fatigue damage calculation, the same definition of fatigue failure has to be applied to the fatigue-life curve tests needed for determination of the set of experi-

mental points  $(\sigma_{ai}; 2N_{fi})_{i=1}^n$  (Fig. 2), used for calculating material constants  $\sigma_f'$ ,  $b$  in accordance with the methodology in Section 2. There could be a wide difference between the fatigue-life curves determined for the number of cycles that cause total fracture of the test specimen and those that initiate cracks. Application of the material constants obtained for the number of cycles to total fracture might lead to an erroneous FLDF estimation. There are several methods for determining the number of cycles to “*engineering crack initiation*”, e.g. continuous monitoring of the test specimen by a camera system, continuous monitoring of the stress response (under the  $\varepsilon_a = \text{constant}$  loading mode), and others. The method, presented in [31], is among the latest developed to detect the initiation of fatigue cracks during fatigue testing.

In fatigue-reliability assessment the values of  $L_g$  calculated for the small values of  $P_a$  are important (Fig. 1). These values greatly depend on the value of the standard deviation  $s_N$ , as is evident from Fig. 9. In our case ( $s_N = 0.213$ ), for the  $P_a$  of 5% we can guarantee a fatigue life of only 3.6 years. Increase in the scatter of experimental points on the fatigue-life curve in Fig. 4 (e.g. consequent to deterioration in quality of welding) would reduce this fatigue life further. For instance, by increasing the standard deviation to a value of  $s_N = 0.4$  for the  $P_a$  of 5%, we can guarantee a life of only 1.8 years and for  $P_a$  of 1% of only 0.94 years (Fig. 9, Table 4). From this point of view, the critical spot investigated in the vehicle's construction seems vulnerable to material fatigue.

It follows from the reasons given above, that the magnitude of scatter greatly influences the operational

reliability of the construction (from the material fatigue point of view). The greater the magnitude of the scatter the longer will be the expected fatigue-life span, which could be a result of the scatter of the material's cyclic properties. Ideally, i.e. at zero scatter (when all experimental points in Fig. 4 are situated on the regression line), the fatigue life of the construction would equal the value of  $FL(50\%) = 8.02$  years, Fig. 7. However, for a standard deviation of  $s_N = 0.4$  this life could dwindle to only 1.8 years (depending upon the value of  $P_a$ , Fig. 1), Fig. 9. To fulfil the requirement for reliable operation  $P_a = 5\%$  and  $L_{req} = 5$  years the standard deviation should be  $s_N \leq 0.12$ . Therefore, minimizing scatter of the cyclic material properties at the critical spot of the vehicle's construction improves the fatigue reliability of the vehicle, e.g. by adopting a different welding technique, by selection of a material with better fatigue properties, etc.

## 6. Conclusions

The magnitude of scatter of the cyclic material properties (represented by the standard deviation of the distribution of number of cycles to fatigue failure on the  $S-N$  curve) is a parameter of crucial importance and considerably influences the fatigue reliability of the construction.

Therefore, a simple computing method has been proposed for the determination of characteristics of materials, namely the fatigue strength coefficient (exponent)  $\sigma_f'(b)$  and fatigue ductility coefficient (exponent)  $\varepsilon_f'(c)$ , for any probability of occurrence.

The proposed procedure of probabilistic interpretation of material characteristics, representing material's cyclic properties, was built into the model for fatigue-life estimation under random loading. The modified model of life estimation (Fig. 3) enables calculation of the fatigue-life distribution function (FLDF) in respect of the scatter of cyclic properties of the material.

The estimation model of FLDF enables to solve various dilemmas in the field of fatigue reliability of the constructions. The model is especially useful not only in the design stage, but also in assessing the fatigue reliability of existing constructions. Where the operational endurance value ( $L_{req}$  in Fig. 1) is required, the model enables:

- calculation of the probability of occurrence of premature fatigue failure of the construction for different load conditions (different loading macroblocks entering the life calculation);
- optimizing selection of the material of construction in terms of the desired operational endurance ( $L_{req}$ , Fig. 1) and permissible probability of occurrence of premature fatigue failure ( $P_a$ , Fig. 1);
- comparing effectively the different design con-

cepts of the critical spot of the construction keeping fatigue reliability in view;

- comparing different methods of welding and heat-treating processes;
- assessing new requirements for failure-free operation of the construction for varying service conditions (by enabling calculation of FLDF for new load conditions and consideration of another  $L_{req}$  value in fatigue reliability assessment).

Potentialities of the estimation model of FLDF were demonstrated by evaluating the fatigue reliability of an urban vehicle's construction. It has been shown that the magnitude of scatter greatly influences the operational reliability of the construction, e.g. for the requirement of 5 years of failure-free operation the probability of premature fatigue failure varies from 2.5% to 30%, depending upon the magnitude of scatter.

## Acknowledgements

This work received financial support from the Slovak Research and Development Agency under the contract APVV-0437-07, Scientific Grant Agency of the Ministry of Education of the Slovak Republic and the Slovak Academy of Sciences under the contract VEGA 2/7086/27 and from the Ministry of Education and Youth of the Czech Republic under the contracts MSM4771868401 and 1M0519.

## References

- [1] MANSON, S. S.: Behavior of materials under conditions of thermal stress. Heat Transfer Symposium. Ann Harbor, Michigan, University of Michigan Engineering Research Institute 1953, p. 9.
- [2] COFFIN, L. F.: Trans. ASME, 76, 1954, p. 931.
- [3] BASQUIN, O. H.: American Society for Testing and Materials, Proceedings 10, 1910, p. 625.
- [4] LANDGRAF, R. W.—MITCHEL, M. R.—LAPOINTE, N. R.: Monotonic & Cyclic Properties of Engineering Materials. Metallurgy Department, Scientific Research Staff. Dearborn, Michigan, Ford Motor Company 1972.
- [5] KUČERA, J.—TALPA, I.—BRÁZDA, H.: Strojírnoství, 34, 1984, p. 690 (in Czech).
- [6] Code of practice for fatigue design and assessment of steel structures. British Standard BS 7608, 1993.
- [7] PALMGREN, A.: ZVDI, 68, 1924, p. 339.
- [8] MINER, M. A.: Journal of Applied Mechanics, 67, 1945, A159.
- [9] KLIMAN, V.: Mater. Sci. & Engng., 68, 1984, p. 1.
- [10] FATEMI, A.—YANG, L.: Int. J. Fatigue, 20, 1998, p. 9. doi:10.1016/S0142-1123(97)00081-9
- [11] MATSUIISHI, M.—ENDO, T.: Japan Society of Mechanical Engineers, 2, 1968, p. 268.
- [12] AMZALLAG, C.—GEREY, J. P.—ROBERT, J. L.—BAHUAUD, J.: Int. J. Fatigue, 16, 1994, p. 287. doi:10.1016/0142-1123(94)90343-3

- [13] KLIMAN, V.: Kovove Mater., 36, 1998, p. 419 (in Slovak).
- [14] MORROW, J. D.: Fatigue Properties in Metal. Fatigue Design Handbook. Advances in Engineering. Vol. 4. Ed.: Graham, J. A. Warrendale, PA, Society of Automotive Engrs. 1968.
- [15] GOODMAN, J.: Mechanics Applied to Engineering. Vol. 1. 9th ed. London, Longmans 1931, p. 634.
- [16] SODERBERG, C. R.: Trans. Am. Soc. Test Matls, 52, 1930, p. 13.
- [17] GERBER, W.: Bestimmung der zulossigne Spannungen in eisen Constructionen. Z Bayer Arch Ing Ver 1874, p. 6.
- [18] SMITH, K. N.—WATSON, P.—TOPPER, T. H.: JMLSA, 5, 1970, p. 767.
- [19] LUKÁŠ, P.—KUNZ, L.: Int. J. Fatigue, 11, 1989, p. 55.
- [20] NIHEI, M.—HEULER, P.—BOLLER, CH.—SEEGER, T.: Int. J. Fatigue, 8, 1986, p. 119. [doi:10.1016/0142-1123\(86\)90002-2](https://doi.org/10.1016/0142-1123(86)90002-2)
- [21] GOLOS, K. M.: Mater. Sci. & Engng., A111, 1989, p. 63.
- [22] WEHNER, T.—FATEMI, A.: Int. J. Fatigue, 13, 1991, p. 241. [doi:10.1016/0142-1123\(91\)90248-W](https://doi.org/10.1016/0142-1123(91)90248-W)
- [23] KWOFIE, S.—CHANDLER, H. D.: Int. J. Fatigue, 23, 2001, p. 341. [doi:10.1016/S0142-1123\(00\)00098-0](https://doi.org/10.1016/S0142-1123(00)00098-0)
- [24] LAGODA, T.—MACHA, E.—PAWLICZEK, R.: Int. J. Fatigue, 23, 2001, p. 283. [doi:10.1016/S0142-1123\(00\)00108-0](https://doi.org/10.1016/S0142-1123(00)00108-0)
- [25] XIA, Z.—KUJAWSKI, D.—ELLYIN, F.: Int. J. Fatigue, 18, 1996, p. 335. [doi:10.1016/0142-1123\(96\)00088-6](https://doi.org/10.1016/0142-1123(96)00088-6)
- [26] BERGMAN, J. W.—SEEGER, T.: VDI-Report of Progress, 18, 1979, p. 6.
- [27] KLIMAN, V.—FÜLEKY, P.—JELEMENSKÁ, J.: Residual Operating Fatigue Lifetime – Estimation of Distribution Function. In: Advances in Fatigue Lifetime Predictive Techniques. 3<sup>rd</sup> Vol. Eds.: Mitchell, M. R., Landgraf R. W. ASTM STP 1292. West Conshohocken, PA, American Society for Testing and Materials 1996, p. 305. [doi:10.1520/STP16144S](https://doi.org/10.1520/STP16144S)
- [28] HEULER, P.—SEEGER, T.: Int. J. Fatigue, 8, 1986, p. 225. [doi:10.1016/0142-1123\(86\)90025-3](https://doi.org/10.1016/0142-1123(86)90025-3)
- [29] SUSMEL, L.—ALIABADI, F. M. H.—TOVO, R.—LIVIERI, P.: Int. J. Fatigue, 31, 2009, p. 1. [doi:10.1016/j.ijfatigue.2008.05.021](https://doi.org/10.1016/j.ijfatigue.2008.05.021)
- [30] RADAJ, D.—SONSINO, C. M. P.—FRICKE, W.: Int. J. Fatigue, 31, 2009, p. 2. [doi:10.1016/j.ijfatigue.2008.05.019](https://doi.org/10.1016/j.ijfatigue.2008.05.019)
- [31] KRŠŠÁK, P.: Damage detection of vibrating mechanical systems. [PhD thesis]. Bratislava, Slovak University of Technology in Bratislava, Faculty of Mechanical Engineering 2008, p. 92 (in Slovak).

## Appendix

Material constants ( $\sigma'_f$ ,  $b$ ), computed for different probability of occurrence  $P\%$  (Fig. 2)

Regression line (Fig. 4, Eq. (16)) $\sigma_a = 787.34 (2N_f)^{-0.22921}$		log-normal distribution $s_N = 0.213$		
$P$ (%)	$(d_{(P\%)})$ below/ <b>above</b> regression line	$\sigma'_f$ (MPa)	$b$ (–)	
1	2.330	605.90	–0.22921	
5	1.640	654.77	–0.22921	
10	1.280	681.82	–0.22921	
30	0.524	742.30	–0.22921	
<b>50</b>	<b>0.000</b>	<b>787.34</b>	<b>–0.22921</b>	
70	<b>0.524</b>	835.11	–0.22921	
90	<b>1.280</b>	909.18	–0.22921	
95	<b>1.640</b>	946.73	–0.22921	
99	<b>2.330</b>	1023.09	–0.22921	